University of Szeged

Faculty of Pharmacy

Institute of Pharmacodynamics and Biopharmacy

PhD. Thesis Summary

Evaluation of the oncopharmacological potentials of the novel A-ring modified 13α-estrone derivatives

Hazhmat Ali

Supervisor:

Professor Dr. István Zupkó

Szeged, 2023

University of Szeged

Doctoral School of Pharmaceutical Sciences

Pharmacodynamics, Biopharmacy and Clinical Pharmacy PhD Program

Program director: Professor Dr. István Zupkó

Hazhmat Ali

Evaluation of the oncopharmacological potentials of the novel A-ring modified 13α-estrone derivatives

Supervisor: Professor Dr. István Zupkó

Complex Exam Committee:

Chairman: Prof. Dr. István IIisz
Members: Prof. Dr. György Balogh
Prof. Dr. Anna Borsodi

Final Exam Committee:

Chairman: Prof. Dr. György Dombi
Reviewers: Prof. Dr. Pál Perjési
Prof. Dr. Tamás Csont

I. INTRODUCTION

Cancer is a worldwide progressive health condition that occurs not only due to demographic changes, but also as a consequence of globalization, unhealthy life style and transition in risk factors. Estimation of the global cancer burden in 204 countries from 2010 to 2019 indicated that, cancer was the second cause of death followed by cardiovascular disorders where the largest percentage in morbidity and mortality rates were documented specifically in low income countries. Studies examined the link between human development and cancer incidence concluded that, future cancer burden is expected in less developed countries with a 100% increase until 2030.

In addition to their ordinary hormonal functions, certain estrogens possess other biological activities including neuroprotective, antiangiogenic as well as anticancer effects. Among the estrogens that exhibit the previously mentioned biological effects, is 13α-estrone, which is an isomer of the estrone. The main risk in the design of estrane based anticancer agents is the possible hormonal side effects. The probable mechanism to overcome this obstacle and minimize the undesirable estrogenic activity, is the transformation of natural estrogens into their core-modified analogs. It was shown that inversion in the configuration at C-13 results in a modified conformation, therefore, analogs of 13α-estrone don't possess estrogenic behavior. It is important to mention that certain enzymes involved in estrogen biosynthesis can be inhibited by 2- and/or 4-substitued 13α-estrone derivatives. Moreover, the organic anion transporter protein (OATP2B1), which is one of the key players in intestinal drug absorption and transport, might also be inhibited by certain 13α-estrone derivatives.

Concerning the antiproliferative potential of 13α-estrones, our research group (Zupkó and colleagues) has been studying in vitro investigation for nearly a decade. It was concluded that, certain derivatives display outstanding growth inhibition against a panel of human gynecological adherent cancer cell lines. Investigation of the mechanism of action of certain compounds demonstrated their capability to induce cell cycle blockade at G2/M phase. Some derivatives induced apoptosis via the intrinsic pathway. These data suggest that 13α-estrones are of great value owing to their multiple bioactive affects without estrogenic behavior.

2. AIMS AND OBJECTIVES

Throughout the duration of our experiments, preliminary assessment for numerous novel A-ring modified 13α-estrone derivatives has been performed. Several candidate compounds were identified and the most potent antiproliferative agent was chosen for further evaluation. The aim of the present study was to investigate in vitro antineoplastic properties of the most potent compound against the HPV16 positive human invasive cervical cancer cell line (SiHa) as well as to explore its mechanism of action.

The detailed objectives of the conducted experiments are clarified as follows;

- Assessment of the antiproliferative potential of various 13α-estrone derivatives against a panel of human adherent gynecological cancer cell lines as well as determination of its half maximum inhibitory concentration (IC_{50}) values via MTT assay.
- Estimation of tumor selectivity by measuring the growth inhibitory percentage against non-cancerous mouse fibroblast cell line (NIH/3T3).
- Investigation of the mechanism of action of the selected compound by assessing its influence on cell cycle distribution.
- Determining the ability of the chosen compound to induce morphological changes represented by necrosis and apoptosis using Hoechst 33258/Propidium Iodide fluorescent double staining (HOPI).
- Demonstrating the proapoptotic activity through the colorimetric determination of caspase-3 enzyme activity.
- Determining the effects of the candidate compounds on microtubules thorough performing cell-free tubulin polymerization assay.
- Exploring the antimetastatic capacity particularly on cell migration and invasion by conducting both wound healing and Boyden chamber assays respectively.

3. MATERIALS AND METHODS

3.1. Chemical structures of the novel A-ring substituted 13α-estrone derivatives

A total of 47 newly synthesized 13α-estrone derivatives have been investigated in this study. Modifications were mainly substituted in the A-ring of the hormonally inactive 13α-estrone core. The novel compounds were categorized into 3 sets based on the nature of the substituents introduced. Syntheses of all novel 13α-estrone derivatives was carried out by colleagues of the Institute of Organic Chemistry, University of Szeged, Hungary.

3.1.1 A-ring halogenated 13α-estrones

The first set of compounds (**1**-**17**) represents 3-hydroxy or 3-benzyloxy 2- or 4-(substituted) phenyl derivatives (**Figure 1**). Modifications were applied at positions C-2 and C-4 of the A-ring of the hormonally inactive 13α-estrone core.

3.1.2 Steroidal diaryl ethers

The newly synthesized compounds in this set (**18**-**29**) includes the novel 13α-estrone derivatives arylated directly at the *C*-3-*O* function. The chemical structures are illustrated in **Figure 2**.

3.1.3 Carbamate, sulfamate and pivalate derivatives of 13α-estrone and their 17-deoxy counterparts

The third set of compounds (**30**-**47**) includes newly synthesized 3-*O*-carbamoyl, -sulfamoyl, or –pivaloyl derivatives of 13α-estrone and their 17-deoxy counterparts. The chemical structures of this group of compounds are illustrated below (**Figure 3**).

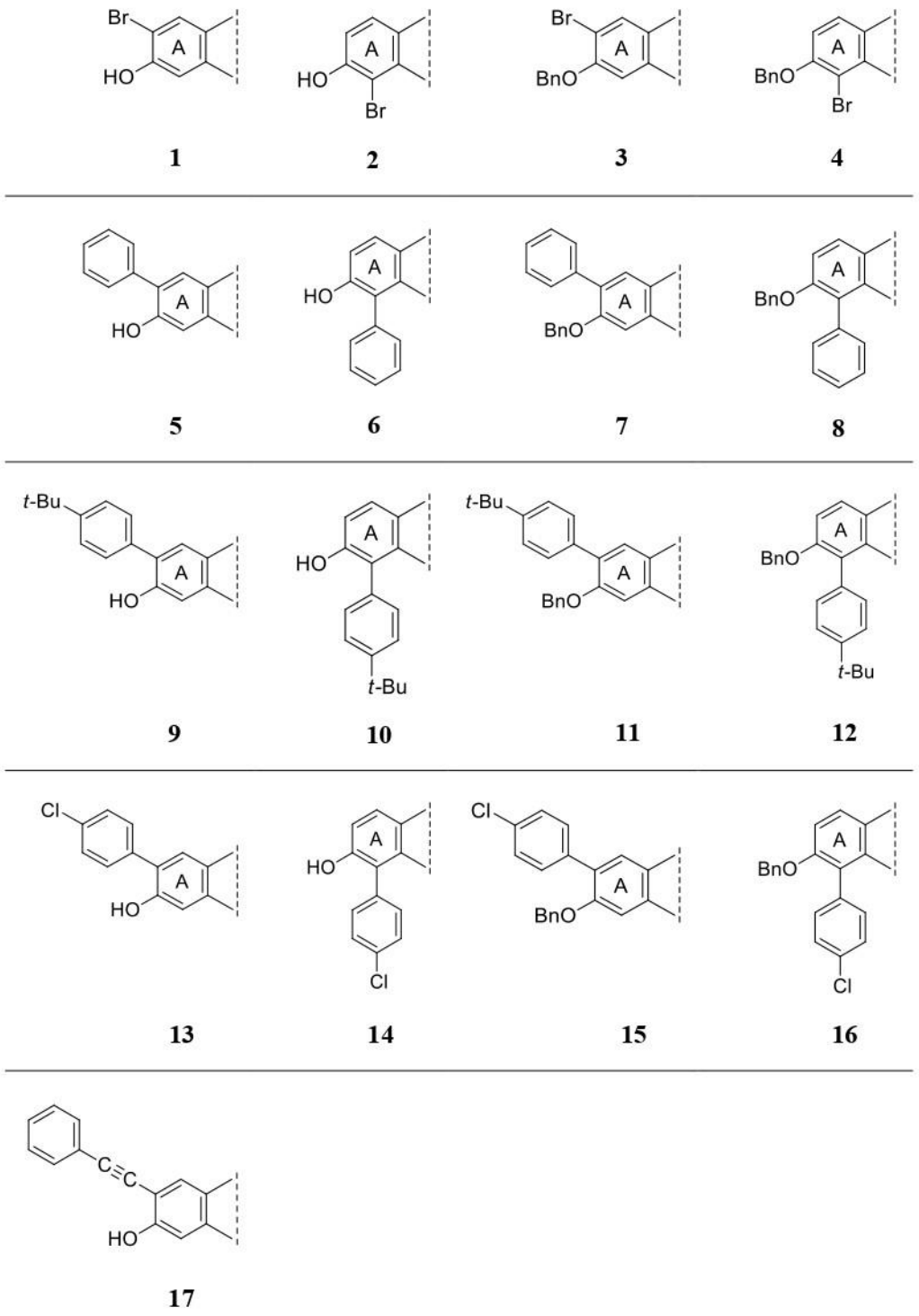

Figure 1: Chemical structures of the A-ring halogenated 13α-estrone derivatives

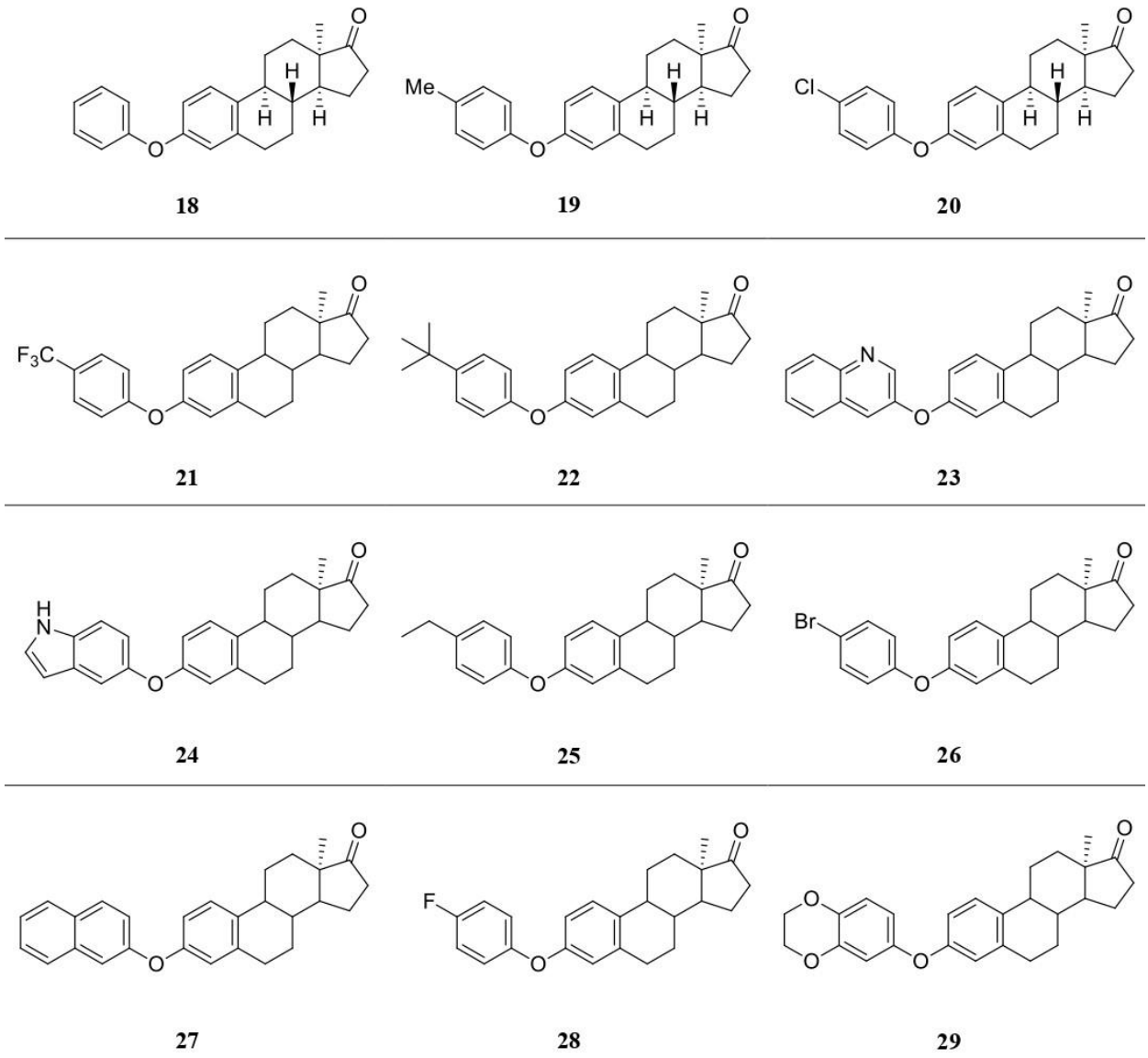

Figure 2: Chemical structures of steroidal diaryl ethers

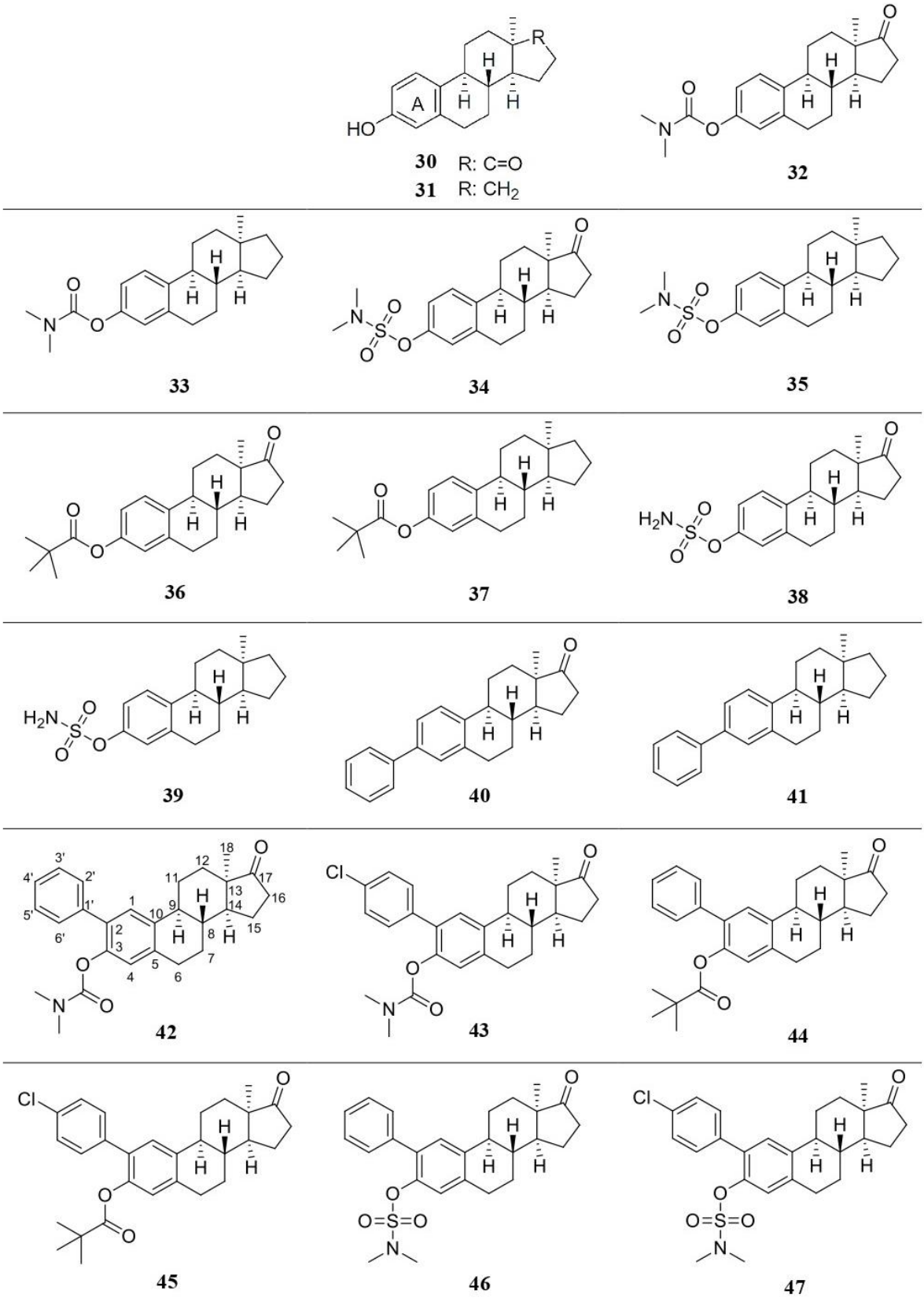

Figure 3: Carbamate, sulfamate and pivalate derivatives of 13α-estrone

3.2. Tumor cell lines and culture

In this study, a panel of human adherent gynecological cancer cell lines were used to conduct in vitro experiments. Breast cancer cell lines (MCF-7, MDA-MB-231), ovarian (A2780), cervical (HeLa) and non-cancerous mouse fibroblast cells were purchased from the European Collection of Cell Cultures, Salisbury, UK. The cervical cancer cell line (SiHa) was obtained from the American Tissue Culture Collection, Virginia, USA. All other mediums, chemicals and supplements were purchased from Lonza group Ltd. T, Basel, Switzerland, unless otherwise specified.

3.3. Antiproliferative assay

The growth inhibitory effects of the test compounds against a panel of previously described cancer cell lines was investigated using the standard MTT assay. Active compounds that elicited more than 50% of inhibition undertook a series of dilutions where the sigmoidal dose response curves were fitted to determine their half maximum inhibitory concentration (IC_{50}) values. Cisplatin (Ebewe Pharma GmbH, Unterach, Austria) was used as a positive control.

3.4. Cell cycle analysis by flowcytometry

To determine the mechanism of action of the selected test compound, cell cycle analysis was conducted to measure the cellular DNA contents of cells using flowcytometry. The samples were analyzed by a FACS caliber flow cytometer where at least 20.000 events per sample was evaluated for each analysis. The obtained data were analyzed using ModFit LT 3.3.11 software (Bedford, Massachusetts, USA).

3.5. Hoechst/propidium iodide fluorescent double staining (HOPI)

Fluorescent staining with DNA-specific dyes was performed to detect the necrotic and apoptotic morphological changes in cells induced by the test compound using HOPI method. In each sample, cell nuclei emitting fluorescence were counted and the intact, necrotic and apoptotic cell proportions were expressed as percentages.

3.6. Caspase-3 activity

To evaluate the pro-apoptotic property of the test compound and its ability to induce the programmed cell death, colorimetric caspase-3 activity was measured using commercially available kit (Abnova, Taipei, Taiwan). The absorbance of the cleaved substrate that is directly proportional to the amount of the active caspase-3 was measured by a microplate reader at 405 nm.

3.7. Tubulin polymerization assay

To assess the influence of the test compound on the microtubular system, cell-free tubulin polymerization assay was performed using commercially available kit (Cytoskeleton Inc., Denver, Colorado, USA). To demonstrate changes in polymerization of tubulin induced by the test compound, a polymerization curve was fitted to the measured data. The highest difference between three absorbance values at two consecutive time intervals was considered as maximum rate of tubulin polymerization (Vmax).

3.8. Cell migration assay (wound healing)

To assess the influence of the test compound on cell migration, a wound healing assay was conducted using specific chambers (ibidi GmbH, Martinsried, Germany). The percentage of cell migration (wound closure %) was calculated based on the photos taken at different intervals (0, 24 and 48 hours) using ImageJ software version 1.53a (National Institutes of Health, Bethesda, MD, USA).

3.9. Invasion assay (Boyden chamber)

The anti-invasive capacity of the test compound was assessed using Boyden chamber assay. Several appropriate images were taken per each sample and the percentage of invading cells was calculated in treated cells compared to non-treated controls.

3.10. Statistical analysis

Statistical data analysis in all cell-based in vitro experiments was done by one way analysis of variance followed by Dunnet test. Data were expressed as mean values ± standard error of mean (SEM) using GraphPad Prism version 5.01 (GraphPad, San Diego, CA, USA). *P* values were calculated to display the statistical differences between study groups. The *P* values < 0.05 and < 0.01 were considered statistically significant and highly significant respectively.

4. RESULTS

4.1 Antiproliferative activity and tumor selectivity of the A-ring substituted 13*α*-estrone derivatives

Among the investigated compounds, the 2-(4-chlorophenyl)-13α-estrone sulfamate (compound **47**) was the most potent antiproliferative compound agent among all tested groups, specifically against HVP16 positive human cervical cancer cell line (SiHa). Therefore, it was selected for further evaluation and to explore its mechanism of action. The tumor selectivity index (TSI) for compound **47** was calculated according to the following equation; $IC_{50[cancerous]}/IC_{50[non\text{-}cancerous]}$. The TSIs (except for HeLa) were less than 1 but more than 0.1 indicating that, this compound has moderate tumor selectivity. **Table 5** demonstrates the calculated tumor selectivity indices for compound **47** versus cisplatin against the utilized cell lines.

Cell lines	**IC_{50} malignant/IC_{50} NIH/3T3**	**IC_{50} cisplatin/IC_{50} NIH/3T3**
MCF-7	0.264	2.140
MDA-MB-231	0.680	7.085
HeLa	0.094	4.603
SiHa	0.112	2.903
A2780	0.441	0.481

Table 1: Tumor selectivity index of compound **47** on the utilized cell lines

4.2. Cell cycle analysis

Cell cycle disturbance was induced at 2 and 4 µM concentrations after 24 hours post treatment. It was characterized by a significant elevation in G2/M cell population in the expense of G0/G1 in a dose dependent manner. Moreover, a significant elevation in hypo-diploid subG1 cell population was observed particularly at a higher concentration (4 µM). The same trend was demonstrated after 48 hours of exposure with the test compound [**Figure 4**].

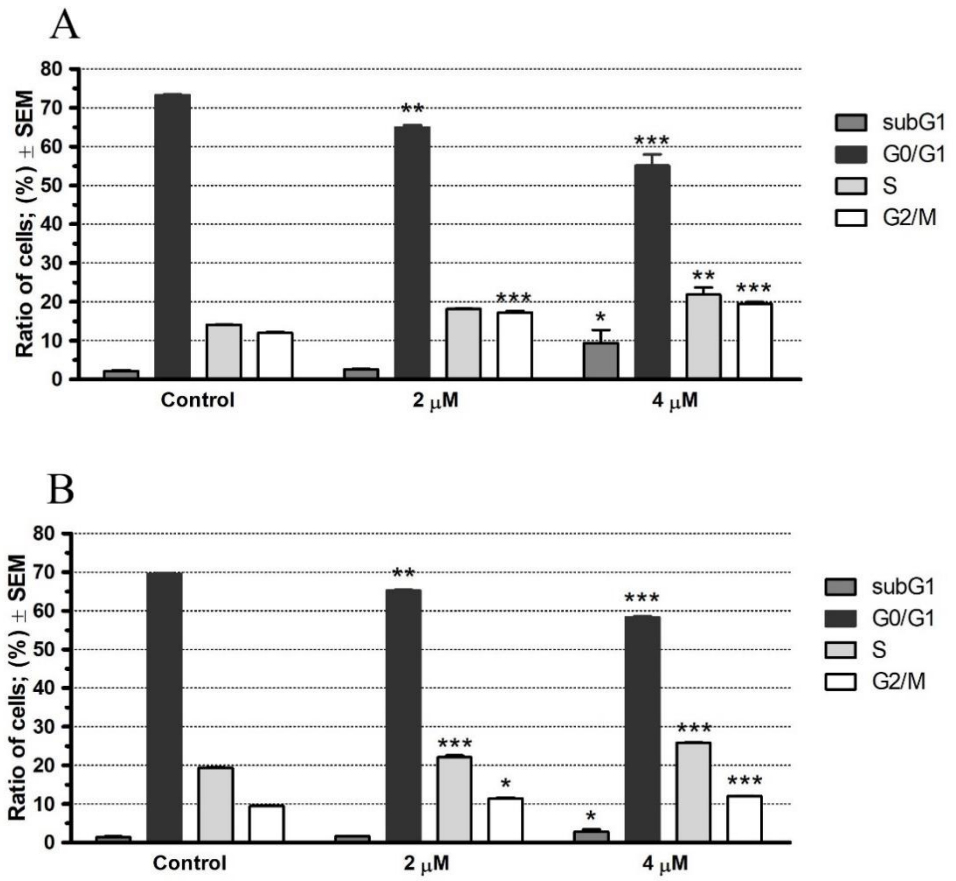

Figure 4. Cell cycle analysis by flowcytometry.

Compound **47** displayed a cell cycle disturbances, characterized by an increased rate of the S and G2/M cell populations at the expense of G0/G1. The upper and lower panels show the effects of **47** on cell cycle phases at 24 (**A**) and 48 (**B**) hours post treatment respectively.

4.3. HOPI fluorescent double staining

Changes in cell morphology and membrane integrity were observed in SiHa cells after 24 hours post treatment. Based on our results, fluorescent images demonstrated a remarkable reduction in viable intact cell population and a significant elevation in cells emitting light blue fluorescence (apoptotic) due to DNA condensation as well as necrotic cells emitting red fluorescent due to damaged cell membrane [**Figure 5**].

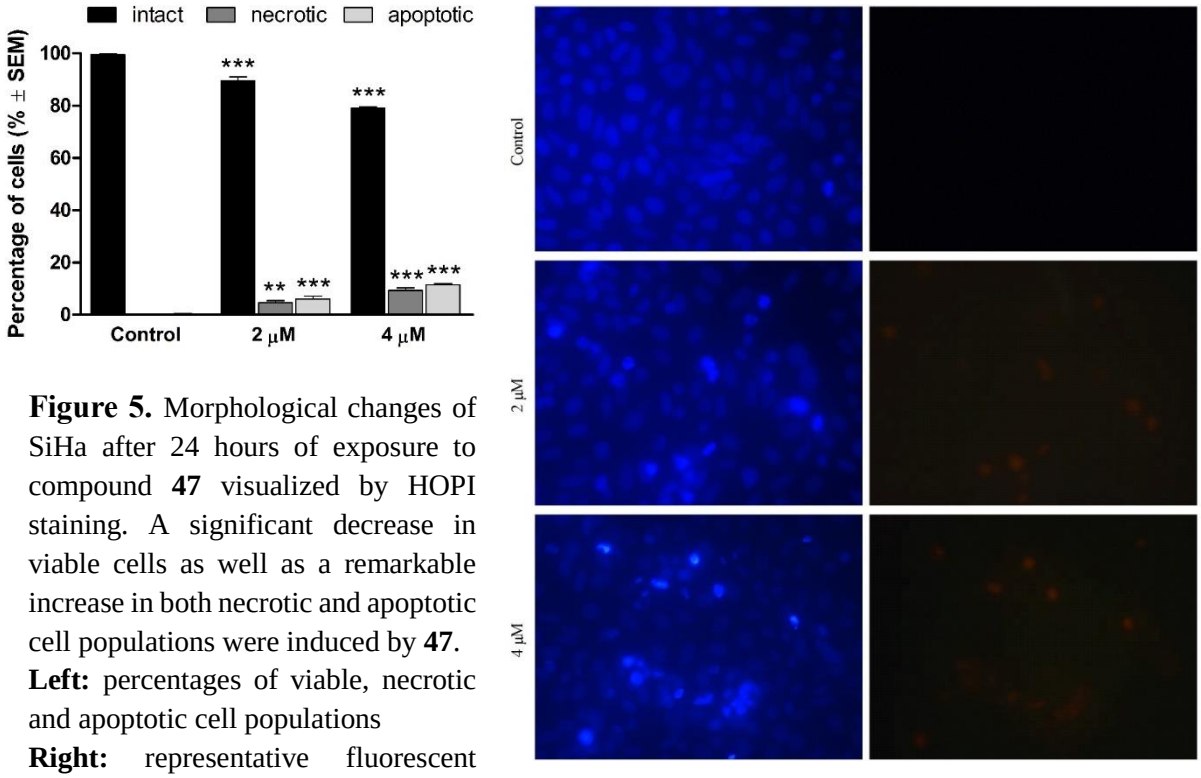

Figure 5. Morphological changes of SiHa after 24 hours of exposure to compound **47** visualized by HOPI staining. A significant decrease in viable cells as well as a remarkable increase in both necrotic and apoptotic cell populations were induced by **47**.
Left: percentages of viable, necrotic and apoptotic cell populations
Right: representative fluorescent images (10x magnification)
** and *** indicate significance at $p < 0.01$ and $p < 0.001$, respectively

4.4. Determination of caspase-3 activity

SiHa cells were treated with 2 and 4 μM concentrations and incubated for 24 hours. A 3-fold increase in caspase-3 enzyme activity was detected after 24 hours of incubation particularly at higher concentration (4 μM) indicating that the apoptosis was induced via the intrinsic pathway [**Figure 6**].

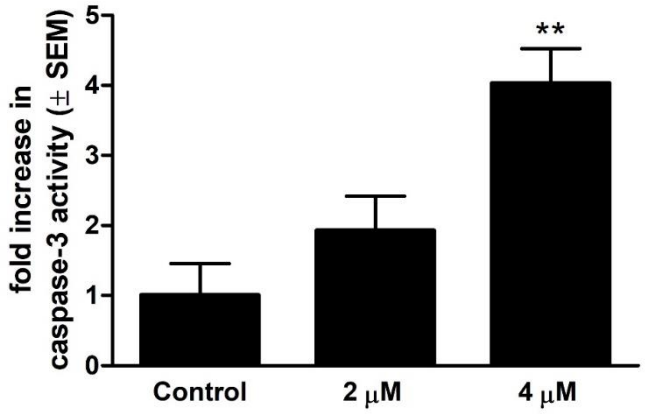

Figure 6. Caspase-3 activity

The proapoptotic property of the test compound was confirmed by assessing caspase-3 activity on SiHa cells after 24 hours post treatment. At a concentration of 4 μM, compound **47** induced a 3-fold increase in caspase-3 enzyme activity compared to untreated control cells.
** indicates significance at $p < 0.01$.

4.5. Tubulin polymerization

A significant increase in tubulin polymerization was induced by all test compounds compared to the negative control. Next, it was essential to calculate the maximum rate of tubulin polymerization (Vmax) for each compound to determine their efficacy of polymerizing tubulin. The calculated Vmax values were statistically significantly higher in all compounds even at lower concentrations, however, they were lower than the reference agent paclitaxel [**Figure 7**]. The obtained data suggest that, the antiproliferative potential of test compounds are elicited through the disturbance of tubulin polymerization.

4.6. Wound healing assay

Compound **47** exerted a statistically significant decrease in cell migration compared to untreated controls after 24 and 48 hours of incubation respectively [**Figure 8**]. The obtained results suggest that, the test compound has potent anti-migratory effects at both 0.5 and 1 μM concentrations.

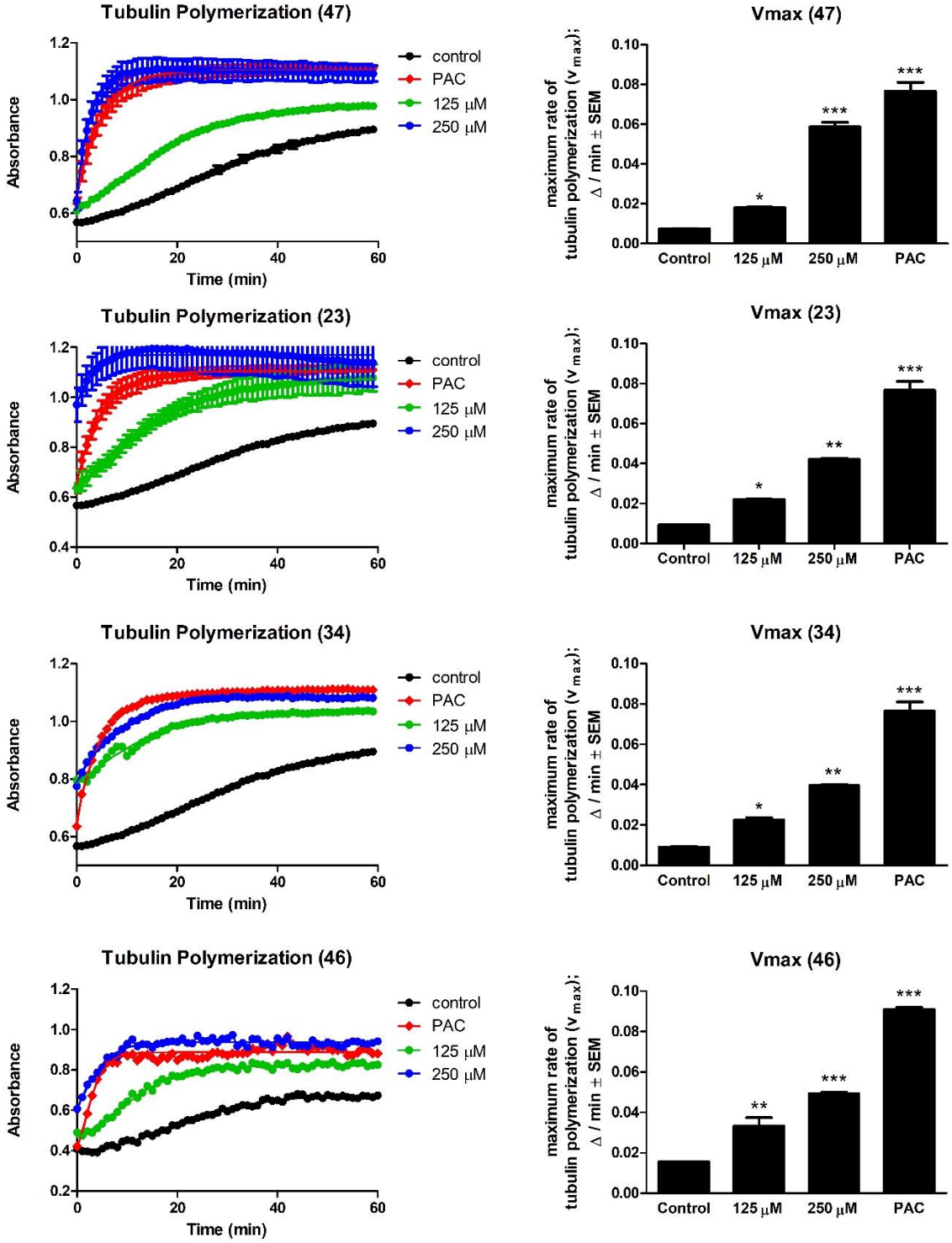

Figure 7: Tubulin polymerization assay. **Left panels**: trends of tubulin polymerization compared to the positive control (paclitaxel 10 µM) and to vehicle. **Right panels**: calculated maximum rates of tubulin polymerization (Vmax). *, **, and *** indicate significance at $p < 0.05$, $p < 0.01$, and $p < 0.001$, respectively.

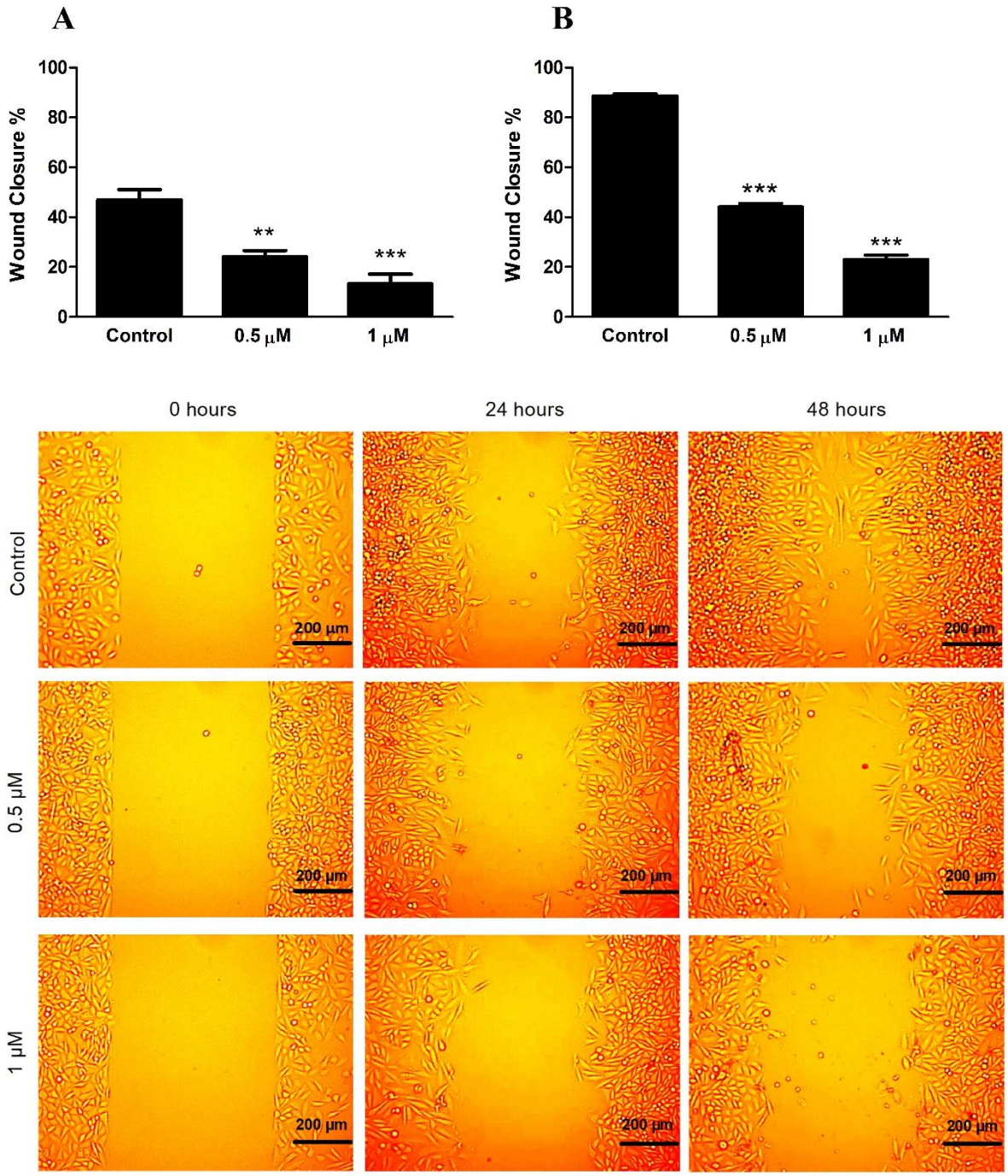

Figure 8: Wound healing assay.

13AOS displayed significant anti-migratory effects on SiHa cells in a dose dependent manner compared to controls.
A and B: Graphs indicate the effects of the test compound on SiHa cell migration after 24 and 48 hours post treatment respectively.
C: Representative images of the anti-migratory effects at 0, 24 and 48 hours post treatment.
Data are presented as mean ± SEM, ** and *** indicate $p < 0.01$ and $p < 0.001$ respectively, compared to control.

4.7. Boyden chamber assay

Based on our results, compound **47** displayed a substantial dose dependent decrease in invasion % compared to untreated samples after 24 hours of exposure [**Figure 9**]. Data suggest that, compound **47** exerted a significant anti-invasive capacity at 0.5 and 1 µM concentrations respectively. Moreover, the anti-invasive effects are obviously starts at 0.5 µM and are substantially lower than the IC_{50} value.

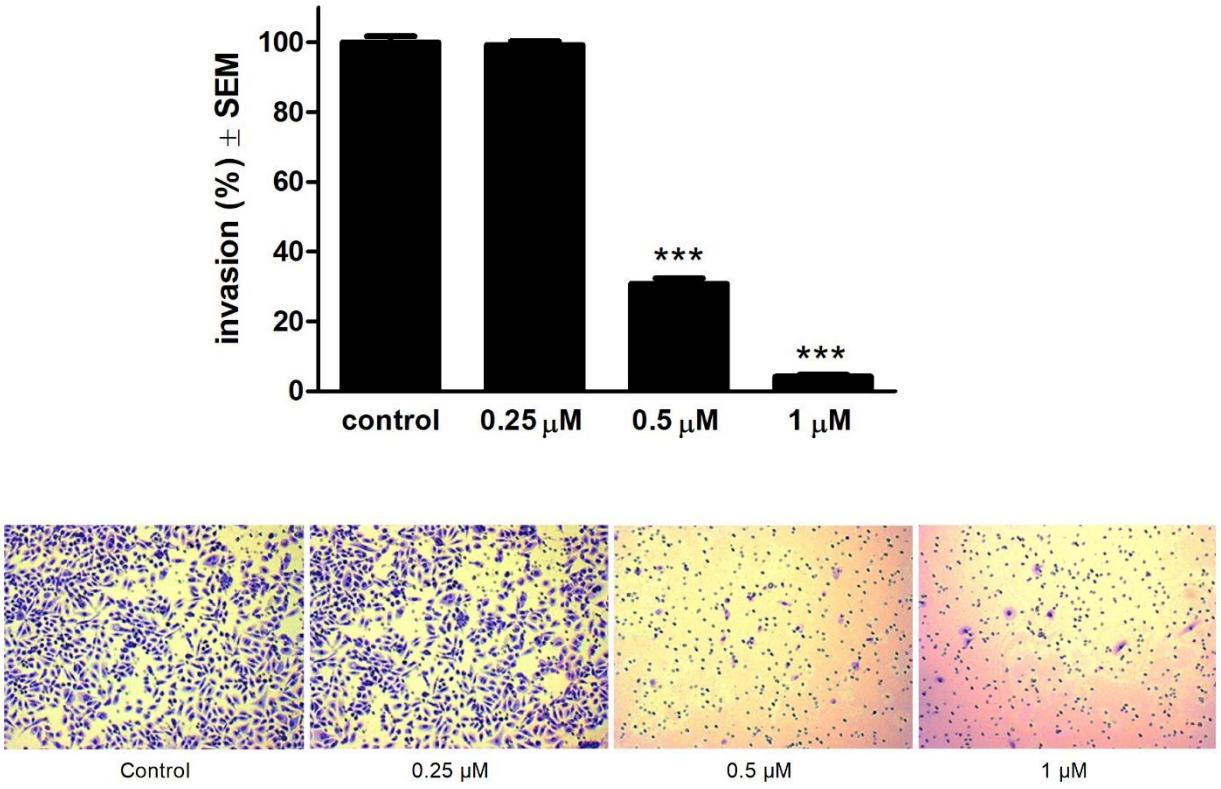

Figure 9: Boyden chamber assay.

Compound **47** elicited a significant anti-invasive effect on SiHa cells, at subantiproliferative concentrations. **Upper panel**: anti-invasive effect of **47** at 24 h post-treatment. *** indicates significance at $p < 0.001$. **Lower panel**: microscopic images showing the density of invasive cancer cells after crystal violet staining (10× magnification).

5. DISCUSSION

The antiproliferative potentials of diverse groups of the core-modified 13α-estrone derivatives have been previously reported by our research group. These modifications were mainly substituted at positions C-2, C-4 and/or 3-OH of the hormonally inactive 13α-estrone core molecule. Certain compounds displayed remarkable growth inhibitory effects with submicromolar IC_{50} values. It was observed that, nature, size and polarity of the introduced functional groups, prominently influences the growth inhibitory action of the synthesized compounds. In addition, introduction of the benzyl or benzyltriazolyl onto 3-OH significantly improved the antiproliferative action. Therefore, a further attention was paid on testing 13α-estrone core derivatives bearing the above mentioned functions. As a consequence, various novel compounds have been synthesized having both enzyme inhibitory and antiproliferative actions.

In this study, 3 sets of the newly synthesized compounds were tested against a panel of gynecological cancer cell lines. Beginning with the A-ring halogenated derivatives (**1-17**), certain compounds (**4, 13** and **9**) have been identified as potent antiproliferative agents. Among the tested cell lines, the estrogen receptor positive MCF-7 and the HPV18 positive HeLa were considered the most sensitive. None of the promising agents displayed a substantial growth inhibition against NIH/3T3 indicating their tumor selectivity. The most potent compound (**4**) displayed a remarkable antiproliferative activity against all tested cell lines but MCF-7 was considered the most sensitive. However, the most potent phenylated compound (**13**) exerted outstanding growth inhibition against MCF-7 and HeLa. It is worth mentioning that, compounds (**4**) and (**13**) behaved similarly concerning both breast cancer cell lines MCF-7 and MDA-MB-231. However, (**13**) differentiated between two uterine cervical carcinoma cell lines HeLa and SiHa. Based on the above explanation, it can be concluded that, substitution in the A-ring of the 13α-estrone core seems to improve the antiproliferative action.

Next, we investigated steroidal diaryl ethers (**18-29**) that were synthesized via direct arylation at the *C*-3-*O* function as reported previously. Among this group, compound **23** was highlighted as the most potent antiproliferative agent against all the tested cell lines. The substantial improvement in its biological activity could be due to the substitution of a nitrogen heteroatom into the introduced moiety. It should be emphasized that certain newly synthesized agents belong to this group exerted more growth inhibitory potential compared to the reference agent Cisplatin. Moreover, the HPV18 positive HeLa was considered the most sensitive cell line to almost the majority of compounds.

With regards to the last set (**30**-**47**), the carmabate, pivalate and sulfamate derivatives were synthesized by substituting *N*- and/or *O*-containing DGs to the phenolic 3-OH functions of the 13α-estrone and its 17-deoxy counterparts. Within this group, certain potent antiproliferative agents were identified (**34, 46 and 47**) and interesting structural activity relationships were detected. Compound **34** (bearing N, N-dimethyl pharmacophore combined with 17-keto group) displayed a potent antiproliferative action against both MCF-7 and HeLa. Moreover, the cell growth inhibitory potential was substantially improved by introducing 4-cholophenyl moiety onto C-2 position of the A-ring. Both HPV18 and HPV16 positive cervical cells were substantially inhibited by **46** and **47** in a very low micromolar range.

Following identification of the most potent antiproliferative agent, it was also essential to determine its tumor selectivity. For that purpose, **47** was tested against the non-cancerous mouse fibroblast cell line (NIH/3T3). The growth inhibition % was not more than 50 even at a higher concentration (30 μM). Furthermore, the tumor selectivity index (TSI) was measured to determine the selectivity status of the candidate compound. The TSI was recorded less than 10 but more than 1 indicating that, our candidate compound (**47**) has moderate tumor selectivity.

Identifying the mechanism of action of the newly synthesized candidate drugs, is considered a crucial step in pharmaceutical research. Based on this concept, we attempted to demonstrate the effects of compound **47** on cell cycle distribution. The test compound was able to induce cell cycle disturbance characterized mainly by a statistically significant elevation in both G2/M and S phases in the expense of G0/G1 cell population. It is worth mentioning that, elevation of subG1 cell population particularly at a higher concentration was also noticed providing a preliminary clue regarding the capability of compound **47** to induce apoptosis.

To investigate the ability of compound **47** to induce apoptosis and to study the morphological alterations upon necrosis and apoptosis, the treated SiHa cells were stained with fluorescent Hoechst and PI double staining. A significant reduction in viable cells as well as a significant increase in both necrotic and apoptotic cell populations was noticed. These data suggest that our test compound exhibits proapoptotic effects.

Understanding the mechanism of apoptosis is a crucial step in determining the precise approach by which a drug exerts its proapoptotic effects. The significant fold increase in caspase-3 enzyme activity in our treated SiHa cells 24 hours post treatment suggests that, compound **47** could induce apoptosis via the intrinsic pathway.

Since the cell migration and invasion are considered key players in metastasis, the in vitro antimetastatic properties of our test compound was assessed using wound healing and Boyden chamber assays. As previously described, compound **47** substantially inhibited cell migration in a dose dependent manner after 24 and 48 hours of exposure. Moreover, it also displayed dose and time dependent anti-invasive effects in micro molar ranges compared to untreated samples. Based on the obtained data, it can be concluded that, compound **47** exhibit potent antimetastatic effects even at very low concentrations.

To explore the effects of our test compounds on MTs, computational simulations were conducted to investigate the ligand binding character to the taxoid binding site. Based on these protein-ligand interaction results, compounds **23**, **34**, **46** and **47** were chosen as candidate agents for tubulin polymerization assay (TPA). As expected, all the four compounds displayed a disturbance in tubulin polymerization characterized by increase in the maximum rate of tubulin polymerization (Vmax). This trend was concentration-dependent even at the lower concentration. Accordingly, it can be concluded that, compounds **23**, **34**, **46** and **47** exert potent effects on microtubular system through stabilizing microtubules. Moreover, the antiproliferative properties of these compounds may be elicited through disturbance of tubulin polymerization.

6. SUMMARY

As concluding remarks, the main findings in this study can be summarized below;

- Among all the tested groups of the A-ring modified 13α-estrone derivatives, compound **47** was highlighted as the most potent antiproliferative agent. It exerted an outstanding growth inhibitory effects against the HPV16 positive human invasive uterine cervical cancer cell line (SiHa) in a micromolar range (IC_{50} = 2.71 µM).
- The tumor selectivity index was between 0.1-10 indicating moderate tumor selectivity.
- The mechanism of action of the candidate agent (**47**) was investigated by cell cycle analysis using flowcytometry. Cell cycle disturbance was induced characterized by increase in the G2/M and S phases in the expense of the G0/G1 cell population.
- Based on the significant elevation in subG1 population in cell cycle analysis, the proapoptotic effects were further evidenced by Hoechst/PI fluorescent double staining as well as caspase-3 measurement. It was indicated that, compound **47** was able to induce apoptosis via the intrinsic pathway.
- The antimetastatic capacity was determined by cell migration and Boyden chamber assays. Compound **47** demonstrated potent antimetastatic properties even at submicromolar ranges.
- Tubulin polymerization assay indicated that, compounds **23**, **34**, **46** and **47** possess direct effects on the microtubules through disturbance of tubulin polymerization. Moreover, the antiproliferative effects may be elicited through increase in maximum rate of tubulin polymerization.

  To the best of our knowledge, compound **47** is considered the first known 13α-estrone derivative with such a high potency against SiHa described in the literature. Therefore, it should be considered as a model for designing new anticancer agents targeting cervical carcinomas.